Discrete element modelling to compute drag coefficients of obstacles impacted by granular flows

Lionel FAVIER, Dominique DAUDON[1], Frederic DONZE, Jacky MAZARS
3SR- Université de Grenoble - France

ABSTRACT: Passive protection structures against natural granular flows (snow avalanches, debris flow) are designed with a rough approximation of their drag coefficient. The purpose of this research is thus to propose numerical tools, based on the discrete element method (DEM), that are able to offer possibilities that include: replicating inner flow properties, overcoming experimental limitations, and calculating the "real" drag coefficient of a granular flow. This numerical model will be validated by means of a laboratory experiment on a free surface glass bead flow impacting a small obstacle. After characterising the zone of obstacle influence and performing a time calculation optimisation, large-scale parametric studies will be presented. Both numerical and physical parameters, such as obstacle geometry and the Froude number, will be explored herein. Lastly, an inter-grain cohesion law will be implemented and its influence on the zone of influence discussed.

KEYWORDS: granular flow, discrete element, obstacle, drag coefficient.

1. INTRODUCTION

Given the importance of material strains, it is typically necessary in the case of granular flows to apply adapted numerical tools. The discrete element method allows for naturally modelling a granular material characterised by major internal movement. This method serves to establish a discrete approach to the problem and was first developed to model molecules or atoms by focusing on particulate matter [ALD 59]. Its 2D application to granular soil was then proposed by Cundall and Strack [CUN 79]. Calculation capabilities were relatively limited at the time, hence simulations were only possible with a reduced number of grains, i.e. from 50 to 1000 at the beginning of the 1980's [AND 80]. Assisted by the evolution in computer capacities, this method started to become widely used in the 1990's and is now able to model approximately one million grains of two types: smooth and non-smooth, depending on whether the elementary grains are deformable or not. The non-smooth approach introduces immediate collisions between non-deformable grains and an irregular time discretisation. Event-driven methods, applied to diluted grains according to the kinetic theory of gases [NAM 96, KUM 05] and contact dynamics and then also applied to dense circles [RAD 96, JEA 99], are qualified as non-smooth approaches. The smooth approach is accompanied by a quasi-regular temporal discretisation, with the contacts displaying a duration determined by local contact laws and with grains able to interpenetrate. The majority of methods adopting this approach are considered to be part of the field of molecular dynamics. Their domain of application is quite broad, extending from modelling the static behaviour of concretes, sands or still clays to modelling flows in silos or natural materials [CRO 01, VALLEY 08].

1.1 General algorithm

The general algorithm used for this method comprises three main steps:

1. An assembly of *n* grains, each with its own geometry, positions and velocities, is first created.
2. Once contacts have been detected, the actions exercised on each grain are calculated through a local contact law and, if needed, gravity.
3. Movement equations are then integrated for every grain, a step that allows calculating new positions and velocities.

Step 1 appears once at the beginning of the simulation; afterwards, steps 2 and 3 are repeated at every time interval until reaching the ultimate real time.

1.2 Local inter-grain interaction laws

Behaviour at the global scale is dictated by inter-grain contact laws at the local level. These local laws are often established using a limited number of parameters, yet remain capable of reporting highly varied global behaviour.

[1] *Corresponding author:* Dominique Daudon,
3SR-ENSE3-BP53-38041 Grenoble Cedex France;
Tel: +33 476 827 044; Fax: +33 476 827 043;
e-mail: dominique.daudon@ujf-grenoble.fr

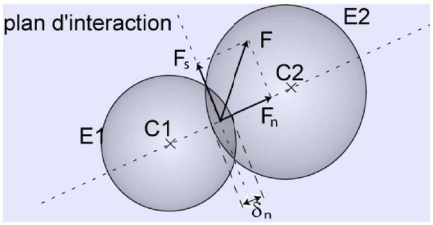

Fig. 1: Contact law of particle E_1 on particle E_2

The contact load between two particles is divided into normal and tangential components, respectively called F_n and F_s (see Fig. 1). The value of F_n may be calculated differently (e.g. in elasticity) as a function of intergranular penetration δ_n. F_s is typically calculated according to a sliding criterion, such as the Mohr-Coulomb criterion [PRO 05]: F_s is dependent upon F_n until reaching a threshold value. Some contact laws may act remotely (when $\delta_n < 0$), which is the case for capillary cohesion [SCH 09]. Various models have been developed for the purpose of modelling adhesive materials, such as metallic powders [LUD 08] or even concrete [SHI 08], by implementing a local attractive force. Granular materials are dissipative [LOU 04], hence this waste can be modelled by adding viscosity [ZHA 98] or a hysteretic phase [WAL 86, FAV 09a]. For further details on the full range of contact laws, the reader is invited to consult [FAV 09b].

1.3 Inclusion of the movement equation

Following calculation of the contact loads exerted on every particle, the incorporation of movement allows computing their new positions and velocities. These equations are based on Newton's second law, which postulates that the sum of forces and moments applied to a discrete particle is equal to the product of its mass multiplied by its acceleration.

1.4 Discrete element method limitations

Most method limitations relate to the time calculation; it is often necessary to adopt a compromise between model representativeness and the time calculation as regards grain shape (generally assumed ideal, i.e. spherical), size and number, or alternatively to adopt simplified local contact laws with respect to reality. For all these reasons, it is essential for numerical models to be experimentally validated before using them as predictive tools.

2. FLOW-OBSTACLE INTERACTION MODELLING

This section of the paper will describe the numerical model of a flow channel developed using the discrete element method by running the YADE code created in the 3SR lab. A completely identical experimental model was simultaneously built for validation purposes, which consists of comparing flow characteristics (velocity profiles, flow height, flow density) with the impact load exerted on an obstacle (more precise information is available in [FAV 09b]).

2.1 Geometry (see Figure 2)

The channel is three-dimensional, with a total length of 2 m (i.e. 1 meter for the flow zone and 1 meter for the 15-litre capacity tank), a width of 20 cm and a height of 15 cm. It is inclined by 43° with respect to the horizontal. The granular material is a nearly monodisperse assembly of spherical glass beads 5 mm in diameter on average. A perpendicular to the 4 cm × 4 cm planar flow obstacle is located at the bottom end of the channel. The flow generated is constantly accelerated beyond the obstacle influence, then slowed to lie within its influence.

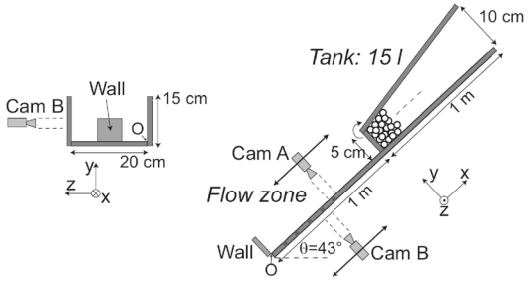

Fig. 2: Experimental set-up and numerical model geometry

2.2 Numerical model validation

The choice of contact law is shown in Figure 3. The normal component is a tri-linear function that represents elastic behaviour, followed by hysteretic and then adhesive [LUD 08].

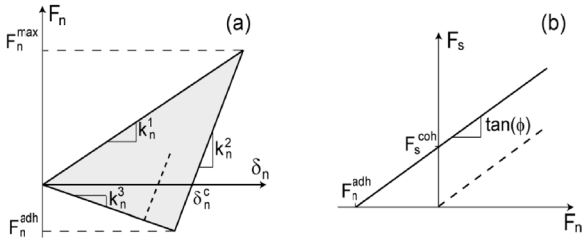

Fig. 3: Local contact laws - Normal component (left) and tangential component (right)

The tangential component follows a sliding Mohr-Coulomb criterion, associated with local cohesion. Dissipation in the contact is characterised by the restitution coefficient $e_n = k_n^1 / k_n^2$ for normal contact and by the friction angle φ for tangential contact. The adhesion characteristic is described by $\alpha_c = k_n^3 / k_n^1$. The higher the value of α_c, the

material becomes more adhesive and thus more cohesive, to a point where the two parameters are linearly correlated through the tangential component. Local parameter values are listed in Table 1.

Type of contact	Grain / grain	Grain / obstacle	Grain / wall
k_n^l (kN.m^{-1})	25	25	2
e_n	0.5	0.5	0.5
α_c	0 - 1	0	0
k_s^l (kN.m^{-1})	5	5	1
φ (°)	30	19	18

Table 1: Micromechanical parameters introduced

To model the experimental set-up on glass beads, both the adhesion and cohesion were reduced to zero. The model could then be validated from: velocity data, thickness, and the impact load exerted by flow in the steady state (Fig. 4). The numerical and experimental data were very similar (5% error), which attests to model validity.

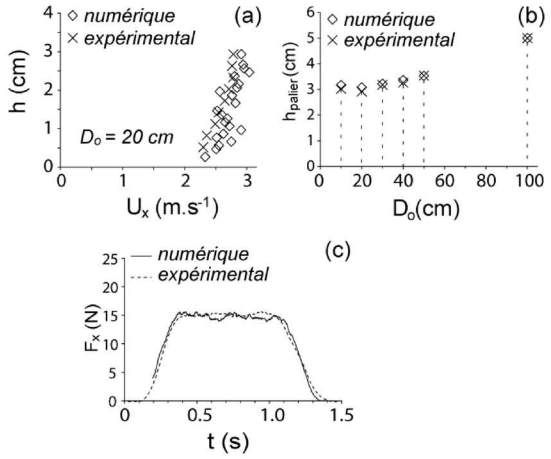

Fig. 4: Comparison of the experimental and numerical velocity flow profile, flow thickness and impact load exerted by flow in the steady state

2.3 Benefit from modelling

Once the model has been validated, it is possible to calculate the properties impossible to measure, such as internal flow characteristics (velocity density), in order to calculate the drag coefficient C_d of the obstacle relative to impact load and flow characteristic. C_d is defined by:

$$C_d = \frac{P_x}{1/2\,\rho U_x^2}$$

with P_x being the pressure exerted on the obstacle, ρ the density, and U_x the flow velocity. This coefficient is commonly introduced to obtain a value of the flow impact stress so as to design the various protective structures. The value of C_d depends on obstacle geometry and flow regime (rapid vs. slow); it is generally defined in the steady state, although an extension is possible to the transient regime if the time evolution of the various flow characteristics involved is known.

3. ENGINEERING APPLICATIONS

3.1 The granular launcher

The previous flow model needs to overcome two weaknesses: calculation time is unacceptable in the case of an engineering-related transfer; and both extensive parametric studies and flow property control procedures are required. Consequently, we propose in this section a simplified numerical approach to the discrete element flow model.

3.2 Granular launcher principle

In the validated standard flow model, considerable time is spent performing the majority of flow tracking since just the interaction with the obstacle is being explored. Sending flow particles from a more accurate position with controlled initial velocity, position and density values could be carried out in order to save calculation time. Only the flow/obstacle interaction zone is investigated. The necessary precondition is that this "launching zone" should lie outside the zone of obstacle influence. The average calculation time for every simulation dropped from 3 days to 6 hours.

The choices of launching distance D_i, initial velocity profile, initial bead density and initial flow height must all be carefully made given that these values need to be as close as possible to those of the standard model, in addition to complying with the C_d calculation hypothesis.

The value of D_i is estimated by two criteria: based on the spatial evolution of velocity over the channel base (Fig. 5a), and on the number of contacts per grain in the flow (Fig. 5b).

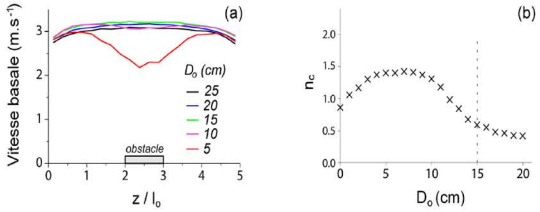

Fig. 5: Launching distance estimation from basal velocity profiles, and mean coordination number of each grain

The first criterion allows us to assert that influence of the obstacle begins between 10 and

15 cm from the obstacle. The second criterion clearly indicates that the coordination number increases significantly below 15 cm from the obstacle. We have thus considered a launching distance D_i equal to 15 cm.

The values of ρ_i, U_i and h_i were extracted from the first model at the centre of the channel, i.e. at a distance D_i from the obstacle. The following parameter values are then obtained: h_i = 3.05 cm, U_i = 3.2 m.s^{-1}, and ρ_i = 1,250 kg.m^{-3}. These values serve as the initial parameter set of the granular launcher and lead to an impact load 6% greater than that produced by the standard model, which is in good agreement when considering validation of the granular launcher for subsequent parametric studies.

3.3. *Influence of obstacle shape*

The influence of two of the most classical obstacle shapes currently considered for flows (Fig. 6) have been studied herein:

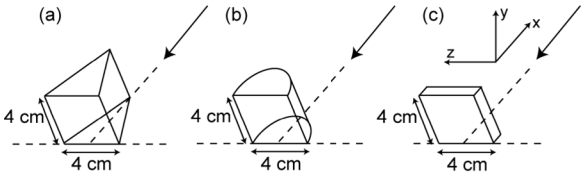

Fig. 6: Obstacle shapes

The parametric study concerns the open angle (Fig. 6a) and curvature (Fig. 6b), respectively. Those cases with an angle equal to 180° and curvature equal to 0 correspond to the limit case of the planar obstacle. On each of the graphs in Figure 7, both the normal and tangential contributions are differentiated within the impact load exerted on the obstacle. The tangential contribution depends on the angle of local friction between the grains and obstacle, set herein at 18°.

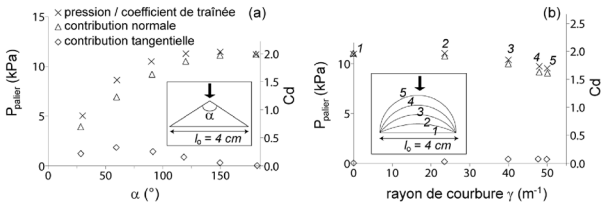

Fig. 7: Impact pressure (normal and tangential contribution), and C_d values for various obstacles in a steady flow state

For the cylinder, the results of pressure and drag coefficient are 15% lower between situations 5 and 1. This value is of the same order of magnitude as that derived from the experimental study on glass bead flow conducted by Hauksson [HAU 07].

3.4 Combined influence of flow regime and adhesion on drag coefficient

The influence of flow regime (slow vs. rapid) with Froude number Fr variation has been studied for the two extreme values of adhesion coefficient a_c = 0 (no adhesion) and a_c = 1 (maximum contact law adhesion) (Fig. 8).

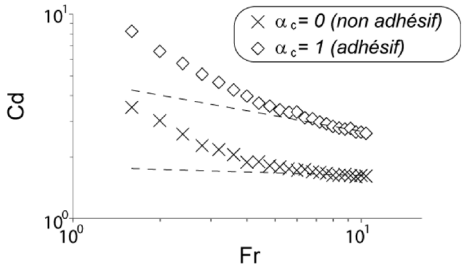

Fig. 8: Drag coefficient function of Froude number for extreme adhesion values
(the classical dense avalanche Froude number varies between 1 and 15 [SOV 08])

In the literature, the evolution of C_d vs. Fr is approximated by a power law function for both snow avalanches [THI 08] and glass bead flows in the laboratory [HOL 04]. Our results present an incomplete power law evolution regardless of the value of a_c. The transition introduces a major contribution of strength bound to slow speed, plus another major contribution of strength bound to gravity, whenever Fr decreases. This hypothesis of a plausible explanation still needs to be confirmed.

Figure 9 shows the contact networks at a given time of the steady state regime for a_c = 0 and a_c = 1. Contact is represented by a bar whose thickness is proportional in the normal contact force intensity. The coordination number increases and the network densifies with adhesion, leading to better transmission of inter-particle loads in the zone of obstacle influence, with the effect of increasing the resultant force exerted, and on the drag coefficient as well.

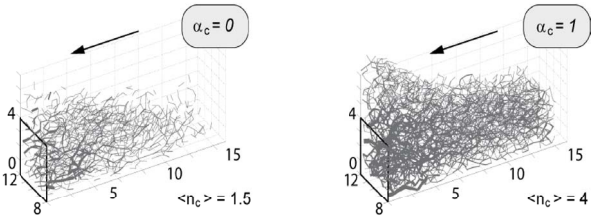

Fig. 9: Contact network for α_c = 0 (zero adhesion) and α_c = 1 (maximum adhesion);
(<nc> refers to the mean coordination number)

4. CONCLUSION

The work conducted has provided a numerical tool, based on the discrete element method, that allows computing the drag

coefficient of obstacles within granular flows. In order to study various shapes and flows, parametric studies have been performed using a granular launcher, offering greater accuracy with respect to the potential calculation time for engineering applications. The selected simplified flow characteristics have in fact slightly overestimated both the drag coefficient and impact pressure in the steady state. Looking to the future, more studies will be undertaken to better understand the transient regime, as well as the formation of the zone of influence and the contact law for snow applications.

REFERENCES

[ALB 99] Albert R., Pfeifer M.A., Barabasi A-L., Schiffer P., "Slow drag in a granular medium", *Physical Review Letters,* Vol. 82, 1999.

[ALD 59] Alder B.J., Wainwright T.E., "Studies in Molecular Dynamics. I: General Method", *Journal of Chemical Physics*, Vol. 31, 1959.

[AND 80] Andersen H.C., "Molecular dynamic simulations at constant pressure and/or temperature", *Journal of Chemical Physics*, Vol. 72, 1980.

[CAL 04] Calvetti F., Di Prisco C., Nova R., "Experimental and Numerical Analysis of Soil-Pipe Interaction", *Journal of Geotechnical and Geo-environmental Engineering,* Vol. 130, 2004.

[COH 95] Coh J.D., Lin M.C., Manocha D., Ponamgi M., "I-collide: An interactive and exact collision detection system for large-scale environments", *Symposium on interactive 3D Graphics*, ACM, 1995.

[CRO 01] Crosta G.B., Calvetti F., Imposimato S., Roddeman D., Frattini P., Agliardi F., "Granular flows and numerical modelling of landslides", *Debris fall assessment in mountain catchments for local end-users*, 2001.

[CUN 59] Cundall P.A., Strack O.D.L., "A discrete numerical model for granular assemblies", *Geotechnique*, Vol. 29, pp. 47-65, 1979.

[FAV 09b] Favier l., Daudon D., Donzé F.V., Mazars J., « Approche numérique par éléments discrets 3D de la sollicitation d'un écoulement granulaire sur un obstacle », *Ph.D. thesis*, Grenoble, 2009.

[FAV 09a] Favier L., Daudon D., Donzé F.V., Mazars J., "Predicting the drag coefficient of a granular flow using the Discrete Element Method", *Journal of Statistical Mechanics: Theory and Experiments*, in press, 2009.

[FRE 06] Freddolino P.L., Arkhipov A.S., Larson S.B., McPherson A., Schulten K., "Molecular Dynamic Simulations of the Complete Satellite Tobacco Mosaic Virus", *Structure*, Vol. 14, pp. 467-449, 2006.

[HAU 07] Hauksson S., Pagliardi M., Barbolini M., Johanesson T., "Laboratory measurements of impact forces of supercritical granular flow against mast-like obstacles", *Cold Regions Science and Technology,* Vol. 49, pp. 54-63, 2007.

[HOL 04] Holzinger G., Hübl J., « Belastung eines Murbrechers: Abgeleitet aus Laborversuchen (Impact forces on a debris flow breaker: derived from laboratory experiments) », *Kongress Interpraevent,* pp. 131-139, 2004.

[JEA 99] Jean M., "The non-smooth contact dynamics method", *Computer Methods in Applied Mechanics and Engineering*, Vol. 177, pp. 235-257, 1999.

[KUM 05] Kumaran V., "Kinetic Model for Sheared Granular Flows in the High Knudsen Number Limit", *Physical Review Letters*, Vol. 95, 2005.

[LUD 08] Luding S., "Cohesive, frictional powders: Contact models for tension", *Granular Matter*, Vol. 10, pp. 235-246, 2008.

[NAM 96] McNamara S., Young W.R., "Dynamics of a freely evolving, two-dimensional granular medium", *Physical Review E*, Vol. 53, 1996.

[PRO 05] Procopio A.T., Zavaliangos A., "Simulation of multi-axial compaction of granular media from loose to high relative densities", *Journal of the Mechanics and Physics of Solids*, Vol. 53, pp. 1523-1551, 2005.

[RAD 96] Radjai F., Jean M., Moreau J.J., Roux S., "Force Distributions in Dense Two-Dimensional Granular Systems", *Physical Review Letters*, Vol. 77, 1996.

[SCH 09] Scholtès L., Chareyre B., Nicot F., Darve F., "Micromechanics of granular materials with capillary effects", *International Journal of Engineering Science*, Vol. 47, pp. 64-75, 2009.

[SHI 09] Shiu W., Donzé F.V., Daudeville L., "Penetration prediction of missiles with different nose shapes by the discrete element numerical approach", *Computers and Structures*, Vol. 86, pp. 2076-2086, 2008.

[SIL 01] Silbert L.E., Ertas D., Grest S., Halsey T.C., Levine D., Plimpton S.J., "Granular flow down an inclined plane: Bagnold scaling and rheology", *Physical Review E*, Vol. 64, 2001.

[SOV 08] Sovilla B., M. Schaer, M. Kern, and P. Bartelt "Impact pressures and flow regimes in dense snow avalanches observed at the Vallée de la Sionne test site", *Journal of Geophysical Research*, Vol. 113, 2008.

[THI 08] Thibert E., Baroudi D., Limam A., Berthet-Rambaud P., "Avalanche impact pressure on an instrumented structure", *Cold Regions Science and Technology,* Vol. 54, pp. 206-215, 2008.

[VAL 08] Valentino R., Barla G., Montrasio l., "Experimental Analysis and Micromechanical Modelling of Dry Granular Flow and Impacts in Laboratory Flume Tests", *Rock Mechanics and Rock Engineering*, Vol. 41, pp. 153-177, 2008.

[WAL 86] Walton O.R., Braun R.L., "Viscosity, Granular-Temperature, and Stress Calculations for Shearing Assemblies of Inelastic, Frictional Disks", *Journal of Rheology*, Vol. 30, pp. 949-980, 1986.

[ZHA 04] Zhang D., Whiten W.J., "Contact modelling for discrete element modelling of ball mills", *Minerals Engineering*, Vol. 11, pp. 689-698, 1998.